

Deep learning for masonry lined tunnel condition assessment

J. Smith & C. Paraskevopoulou

University of Leeds, Leeds, UK

A. Bedi & M. Invernici

Bedi Consulting Ltd., London, UK

ABSTRACT: The condition assessment of masonry lined railway tunnels typically involves manually identifying lining defects from photographic and lidar surveys taken of the tunnel intrados. This process is time-consuming and subjective to the assessor's judgement. However, recent developments in machine learning achieve the quality metrics required to automate the detection of defects from noisy and irregular tunnel data, offering the potential to reduce tunnel assessment and maintenance costs. This paper proposes a deep learning workflow for defect segmentation. The method is evaluated on the task of masonry block segmentation from lidar data. Acceptable performance is achieved on a sample tunnel section, suggesting that similar methods are applicable to other masonry lined tunnel defect segmentation tasks.

1 INTRODUCTION

A reliable railway system is often a key part of a nation's economy and so it is important to prevent railway tunnel failures that may cause system disruptions. Early warning through condition assessments is vital to avoid the significant remediation costs associated with tunnel failure (Paraskevopoulou et al. 2022). However, the majority of railway lines in Great Britain were constructed in the second half of the 19th century and, as a result, most railway tunnels are masonry lined with a deteriorating structure (Atkinson et al. 2021). Built before modern design standards, their behaviour can be challenging to predict. It is therefore important to accurately characterise the serviceability state of each tunnel to enable timely remediation work to take place and prevent a worsening of the structural condition.

At present, the typical masonry tunnel assessment methodology involves a visual and tactile inspection, followed by structural analysis undertaken post inspection in an office setting. In accordance with (NR 2016), a standardised report is produced and defect severities and locations are input into a TCM (Tunnel Condition Marking Index), which generates an overall condition score for the tunnel. The complete inspection and analysis workflow is shown in Figure 1. The following potential tunnel lining defects are considered:

- Spalling
- Open joints or perished mortar
- Water ingress
- Hollow sounding areas
- Bulges or lining deformation, distortion or flattening
- Loose or missing masonry/ block loss
- Cracks and fractures

Each tunnel inspection consists of a team of inspectors traversing the tunnel and visually observing defects using flashlights. Voids behind the tunnel lining may be identified by

tapping the lining with a listening tool, hearing changes in the sound produced. A TLS (terrestrial laser scanning) survey is typically undertaken during an inspection to enable a 3D point cloud of the tunnel to be generated, as many defects can be identified and analysed post-inspection directly from this point cloud.

A manually designed 3D model of the deformed tunnel lining is created using trial and error. Defects including spalling, large cracks and block loss are then visually identified from the offset of the lidar survey from the manually created model. Water ingress and efflorescence can be identified from the RGB data of each point. Thresholding is used to highlight points with outlying properties. Despite the digitisation of the inspection process, the process is still time consuming and dependant on individual assessor's experience, perception, and engineering judgement to locate defects on the 3D model. This can lead to defects being missed. As a result, the benefits from automation are substantial. Despite this, the assessment process has modernised little compared to those within other engineering disciplines.

This paper briefly reviews various literature methods that have the potential to be applied to automate the assessment process, before proposing a deep learning based defect segmentation method. It then analyses the effectiveness of the method when applied to segment tunnel lining masonry blocks from lidar data. This task is chosen, as the non-homogeneity of masonry tunnel linings, partially due to the presence of masonry joints, is a key part of why defect analysis of masonry tunnels is more challenging to automate than concrete lined tunnels. Block segmentation is also a key part of tunnel condition digitisation as it enables individual blocks to have their properties labelled.



Figure 1. Typical tunnel assessment workflow.

2 REVIEW OF ADVANCES IN TUNNEL CONDITION ASSESSMENT

Modernisation of railway tunnel inspection has, in the UK, been mostly limited to the introduction of TLS surveys. Much research has been conducted on the feasibility of robotic inspection methods, including whether sensors can be attached to in-motion rail vehicles. In addition, there are multiple alternative data collection methods that have been proposed to aid inspections including GPR (ground penetrating radar), Muon tomography, and Ultrasound. The field has been previously reviewed by Haack et al. (1995), McCormick (2010), and Strauss et al. (2020). Robotic inspection methods were reviewed by Montero et al. (2015). While many of these methods either simplify the inspection procedure or generate more insightful information about a tunnel's condition, they have generally not been adopted by industry outside of specialist applications. This is often due to the greater upfront cost of new systems and lack of specialist knowledge to operate the machinery and analyse data.

Being able to automatically detect and identify defects from already routinely recorded 2D and 3D sensor data would reduce the cost and subjectivity of the classification process, without requiring additional equipment or specialist personnel. Some have proposed change detection methods such as digital image correlation. Stent et al. (2016), for example, created a workflow to automatically detect concrete tunnel lining changes between subsequent photographic surveys. Changes detected are clustered into groups representing the formation of different types of defect. While the change detection was successful, their defect clustering method produced many false positives and cannot label the nature of each defect cluster.

As reviewed by Spencer et al. (2019), computer vision involving deep learning has been applied extensively for automated defect detection and segmentation across a variety of infrastructure condition assessment tasks. The field of computer vision involves applying algorithms to automatically make conclusions about a scene directly from an image. Since the advent of deep convolutional networks, the field has developed rapidly (Chai et al. 2021). Research has

been conducted, for example by Makantasis et al. (2015), to detect defects in concrete tunnel linings from photos of the tunnel lining using CNNs (Convolutional Neural Networks).

No work could be found extracting defects automatically from masonry lined-tunnels, although studies such as Wang et al. (2018) and Dais et al. (2021) have applied patch based sliding CNN methods for detection of spalling and cracking of external masonry walls from photographic data.

Encoder-decoder based defect segmentation networks such as the U-Net generally achieve higher localisation performance than patch-based ones, so offer the most potential for accurate defect identification from tunnel lining lidar data. They have been successfully applied by Ibrahim et al. (2019) and Loverdos & Sarhosis (2022) to segment masonry joint locations from photographic data of external masonry walls and by Dais et al. (2021) for masonry crack segmentation. These approaches are compared with manual segmentation in Table 1.

The photographic methods used in these studies may be challenging to apply to older masonry lined tunnels, as uniform lighting is difficult and defects are often obscured by significant efflorescence and masonry discolouration. It would be beneficial to use 3D point cloud data recorded by lidar instead of 2D colour image data. A comprehensive lidar survey is also typically already conducted during tunnel inspections. Studies identifying structural defects from 3D point clouds most commonly take a multiview approach. This involves projecting point properties from the sides of a structure's point cloud onto a 2D image. Reducing the complexity of the problem to 2D makes training models easier and takes advantage of the more advanced state of 2D computer vision research. Yoon et al. (2009) conducted early work using geometrical methods to identify concrete tunnel lining defects from lidar data. Defects were defined as points with a significant offset from the plane of the tunnel lining. More recently, patch and encoder-decoder CNNs have been applied to flattened 3D data. Xu & Yang (2020), for example, trained a mask RCNN on photogrammetry data to detect cracks in concrete tunnel linings. Zhou et al. (2021) used a CNN to segment areas of spalling in concrete lined tunnels from 3D point cloud data. To flatten the point cloud, they fitted an ellipse to the inside of the tunnel lining. It is unknown, however, whether lidar generates high enough quality data to be used with machine learning methods on highly non-homogeneous masonry tunnel linings.

Table 1. Infrastructure defect segmentation methods.

Method	Advantages	disadvantages
Manual visual identification	Output is explainable	Time consuming. Output is subjective and often variable.
Change detection methods, for example digital image correlation	Good detection of defects since previous survey, no machine learning required	Requires data from before the formation of defects, Unable to identify defect types
CNN based patch classification	Easy to label data for training	Localisation of defect is limited to size of patch
Encoder-decoder CNN segmentation	Good localisation of defect. Small training sets possible.	Output can be noisy, so often needs post-processing

3 METHODOLOGY

A multiview approach to segment individual masonry blocks from tunnel lining 3D point cloud data is proposed in Figure 2.

The tunnel lining point cloud is first unrolled and flattened onto a 2D plane to enable it to be rasterised without distortion. The transformations for unrolling are calculated from a manually fitted tunnel intrados mesh. Each of the point cloud parameters outlined in Table 2 are then



Figure 2. Proposed block segmentation method.

rasterised onto 2D grids. The rasters are run through a neural network trained to segment masonry joints. Once the mortar has been segmented into a binary image, a watershed algorithm based on the theory outlined in Roerdink & Meijster (2000) is applied to isolate and label each block.

Table 2. Point cloud parameters.

Normal Change Rate
The point cloud normal change rate is a measure of the change in curvature at a certain point, indicating where local surface deviations are present. It is calculated by subtracting the point cloud normal calculated over a small radius from the point cloud normal calculated over a large radius. This is shown in Figure 3a. Point cloud normals are calculated by least squares fitting a plane to points within a radius of the target point using principal component analysis
Surface roughness
This is a measure of a point's deviation from the local surface. A least squares plane is fitted to points within a radius of the target point but excluding the target point. The roughness is the distance of the target point from the calculated plane and is shown in Figure 3b.
Depth map
This is offset of the raw point cloud from the undeformed manually created 3D model.
Intensity
This is the intensity of the reflected laser detected by the lidar scanner. It gives an indication of the reflectance of the surface at the target point
RGB
Colour data is attributed to each point from a camera mounted on the TLS station.

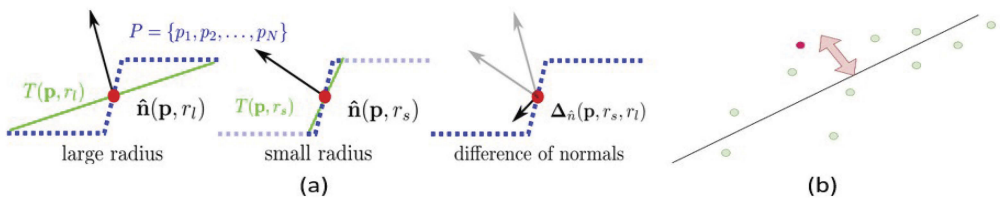


Figure 3. (a) Point cloud normal change rate (b) Point cloud surface roughness.

3.1 Segmentation network

A pixelwise semantic segmentation network is trained on the rasterised images to semantically segment the masonry joints, creating a binary image of their locations. The U-Net and SegAN networks are trialled. The U-Net is a popular Encoder-Decoder format network developed by Ronneberger et al. (2015) that utilises skip connections. Multiple encoders were trialled and a MobileNetv2 encoder was found to be the most effective. Developed by Howard et al. (2017), MobileNet uses depthwise separable convolutions to create a more efficient architecture than encoders such as ResNet. Transfer learning is used by pretraining the encoder on the ImageNet dataset. The Adam optimiser developed by Kingma & Ba (2014) is used in combination with a Binary cross entropy loss function.

The SegAN network developed by Xue et al. (2017) is a generative adversarial network that uses a multiscale objective function. Generative adversarial networks consist of two networks competing in a zero-sum game. One network is an encoder-decoder trained for segmentation, while the other is trained to identify the difference between the segmentation output and the ideal output. This helps the network to perform in a more human-like way and should enable better segmentation of obscured lining areas, for example when adjacent blocks are touching at joints.

3.2 Watershed algorithm

After application of the segmentation network, a marker assisted watershed algorithm is applied to connect gaps in detected joints. This ensures that each block has a complete boundary and so can be individually identified. A similar method was previously used by Ibrahim et al. (2019) for masonry block segmentation from RGB images.

3.3 Network training

Unlike in typical semantic segmentation tasks, the binary masks created for training consist of straight lines representing the masonry joint locations. This is intended to encourage joint location pattern learning and help identify the locations of partially occluded joints.

The network is trained on 512x512 image crops. Five different random transformations are applied to each image and mask pair before each step of training. The transformations Random brightness, Random contrast, Random 90-degree rotation, Random image flip and Gaussian noise were chosen as feasibly realistic. A train test split of 8:2 is used.

3.4 Dataset

A lidar survey of the Sydney Gardens East railway tunnel (SGE) in Bath provided by Bedi Consulting Ltd. was used to evaluate the method and is shown in Figure 4. The tunnel lining is formed of irregularly sized rectangular stone blocks arranged in regular layers of varying sizes. There are substantial mineral deposits causing rough surfaces and obscuring the masonry joints on the intensity and RGB data. Some of the blocks are spalled in places. An 8.5m x 5.25m area of masonry within the northerly part of the tunnel was used for training. After flattening, this section produces a 8486 x 5265 image containing parts of 217 masonry blocks. The training images formed from each of the point cloud attributes outlined in Table 2 are shown in Figure 5. A 0.01m radius was used for normal change rate calculation and 0.1m was used for roughness. A 4-channel method using all the parameters except for RGB was also trialled. A 2397x4286 image of a different part of the tunnel with similar properties was used for testing the optimised networks.

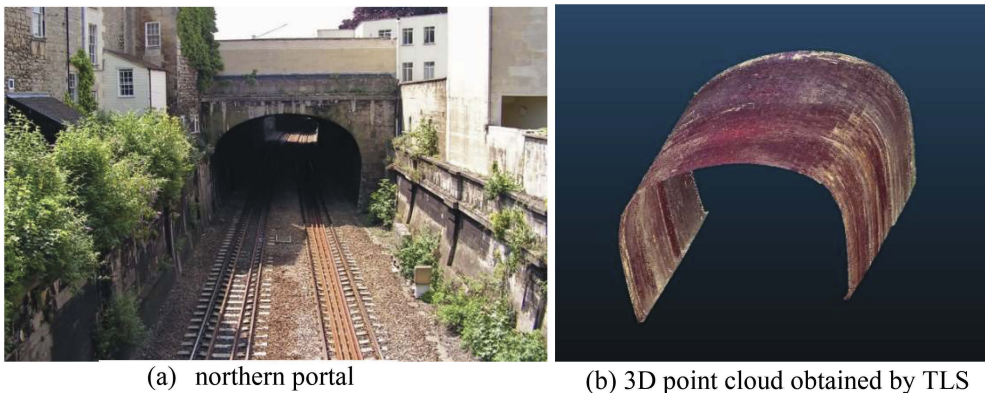


Figure 4. Sydney Gardens East tunnel.

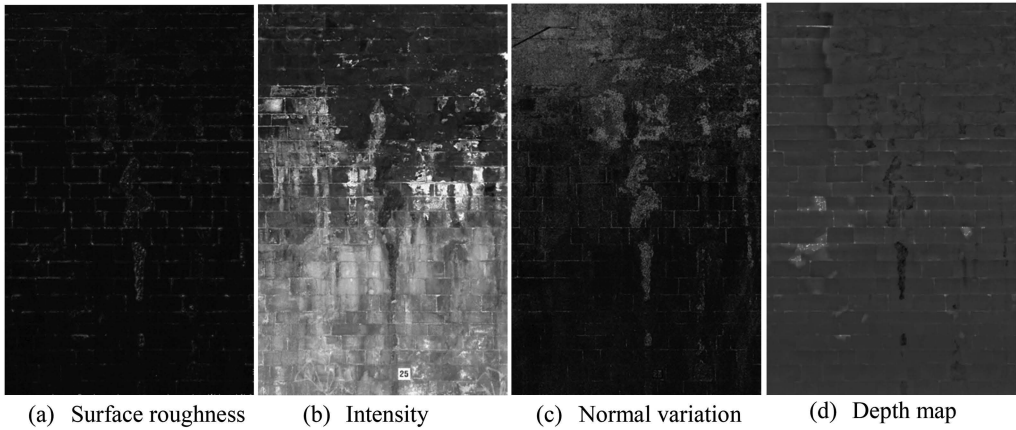


Figure 5. Layers of image used for training.

4 RESULTS & DISCUSSION

The neural networks were trained using PyTorch on an Intel i7 2600k@3.00GHz with 16Gb of RAM. The training utilised CUDA on a Nvidia GTX970 GPU with 4Gb VRAM. Training was conducted for the optimum number of epochs according to validation set results up to a maximum of 200 epochs. The Following hyperparameters were determined as optimal for training:

- Learning rate = 0.0005
- Eps = 1e-08
- Weight decay = 0.00001
- Batch size = 2

The depth map output on the test data is shown in Figure 6. The effectiveness of the U-Net and SegAN networks within the semantic segmentation step is discussed below and recorded quality metrics are shown in Table 3. Where TP = true positive, FP = false positive, and FN = false negative, the following metrics are calculated:

- Precision - This is the percentage of detected joint pixels that are correct and is calculated as $TP / (TP + FP)$.
- Recall - This is the percentage of joint pixels that are correctly identified and is calculated as $TP / (TP + FN)$.
- Intersection over union (IOU) - This combines precision and recall to assess the overall performance. It is calculated as $TP / (TP + FP + FN)$.

Table 3. U-Net and SegAN results.

Image type	Network	Precision	Recall	IOU
intensity	U-Net	0.5515	0.4948	0.3528
normal	U-Net	0.5562	0.4614	0.3373
roughness	U-Net	0.6557	0.4687	0.3761
depth map	U-Net	0.5439	0.819	0.4856
RGB	U-Net	0.2606	0.7000	0.2344
combined	U-Net	0.6381	0.6655	0.4832
intensity	SegAN	0.5646	0.848	0.5128
normal	SegAN	0.5455	0.6836	0.4354
roughness	SegAN	0.583	0.837	0.5235
depth map	SegAN	0.5604	0.8986	0.5271
RGB	SegAN	0.0001	0.4838	0.0001
combined	SegAN	0.5737	0.872	0.5292

In general, an IOU above 0.5 is considered satisfactory performance for segmentation tasks. The depth map obtains the best performance for the U-Net. This is expected, as the image is directly showing the location data of each point and is less impacted by local variations from spalling in the case of the normal variation and roughness images and mineral deposits and water ingress in the case of the intensity and RGB images. The combined 4-channel input is the best SegAN network and also the best network overall, although the performance is not substantially greater than the depth map single channel SegAN network. This suggests that there is not a significant diversity of information between the 4 different non-RGB parameters. RGB data is the worst performer and for the SegAN network could not be effectively trained at all. This is expected, since on the RGB images efflorescence dominates over joint locations. The RGB image is also more complicated, containing many different features. SegAN performs better than U-Net for every image type. This is expected, since the adversarial nature should train the network to generalise better on noisy data.

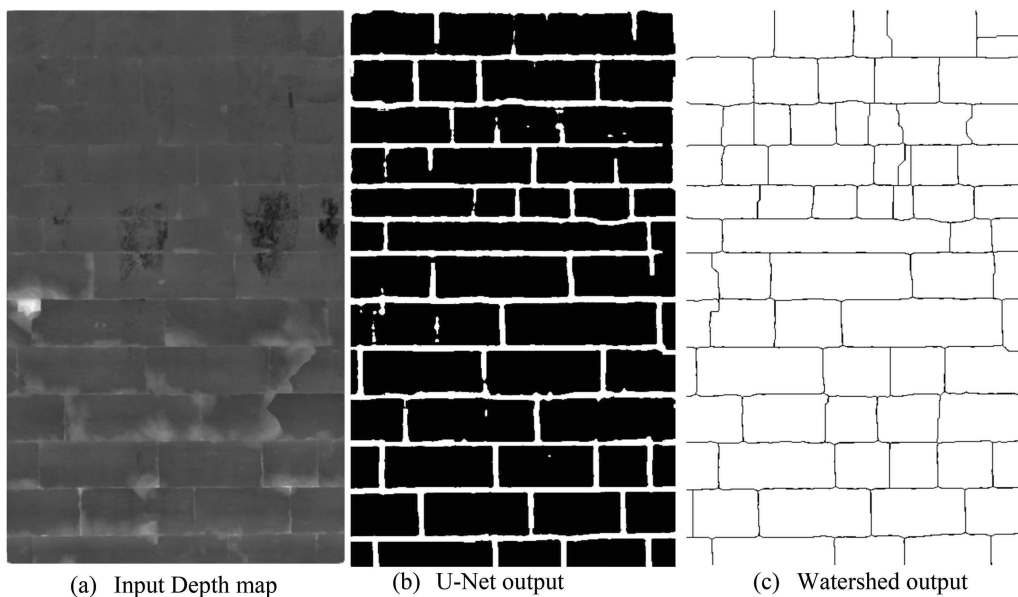


Figure 6. U-Net and watershed output on test data using depth map network.

5 CONCLUSION

While there has been significant research on new tunnel data collection technologies, there has been only limited research on automating the detection and localisation of masonry lined tunnel defects. Encoder-decoder architecture convolutional neural networks that have been successfully applied to semantic segmentation tasks in other fields of engineering have been demonstrated here on masonry lined tunnels. Lidar data of tunnel linings is shown to be of sufficient quality for input to U-Net and SegAN segmentation algorithms. The effectiveness of different point cloud properties for masonry block segmentation was analysed and a 2D depth map was shown to be the most effective input into these segmentation algorithms, although a combined input was also shown to be effective. Further research is necessary to examine how the network would generalise to areas of tunnel lining of different construction types. In addition, it would be useful to compare the effectiveness of 2D multiview with fully 3D computer vision methods including VoxelNet and PointNet. In conclusion, the deep learning based workflow presented may be usefully applied to masonry block segmentation without requiring any additional machinery, expertise or manpower. With sufficient training data, based on results in the literature it also has potential to be applied to segment tunnel lining defects such as spalling.

REFERENCES

- Atkinson, C., Paraskevopoulou, C. & Miller, R. 2021. Investigating the rehabilitation methods of Victorian masonry tunnels in the UK. *Tunnelling and Underground Space Technology*, 108: 103696.
- Chai, J., Zeng, H., Li, A. & Ngai, E.W.T. 2021. Deep learning in computer vision: A critical review of emerging techniques and application scenarios. *Machine Learning with Applications*, 6: 100134.
- Dais, D., Bal, I.E., Smyrou, E. & Sarhosis, V. 2021. Automatic crack classification and segmentation on masonry surfaces using convolutional neural networks and transfer learning. *Automation in Construction*, 125.
- Haack, A., Schreyer, J. & Jackel, G. 1995. Report to ITA Working Group on Maintenance and Repair of underground structures: State-of-the-art of non-destructive testing methods for determining the state of a tunnel lining. *Tunnelling and Underground Space Technology*, 10(4): 413–431.
- Howard, A.G., Zhu, M., Chen, B., Kalenichenko, D., Wang, W., Weyand, T., Andreetto, M. & Adam, H. 2017. MobileNets: Efficient Convolutional Neural Networks for Mobile Vision Applications. *arXiv*. <https://arxiv.org/abs/1704.04861v1> 31 July 2022.
- Ibrahim, Y., Nagy, B. & Benedek, C. 2019. CNN-based watershed marker extraction for brick segmentation in masonry walls. In *ICLAR 2019: Image Analysis and Recognition*. Springer Verlag: 332–344.
- Kingma, D.P. & Ba, J.L. 2014. Adam: A Method for Stochastic Optimization. *3rd International Conference on Learning Representations, ICLR 2015 - Conference Track Proceedings*. <https://arxiv.org/abs/1412.6980v9> 2 August 2022.
- Loverdos, D. & Sarhosis, V. 2022. Automatic image-based brick segmentation and crack detection of masonry walls using machine learning. *Automation in Construction*, 140: 104389.
- Makantasis, K., Protapapadakis, E., Doulamis, A., Doulamis, N. & Loupos, C. 2015. Deep Convolutional Neural Networks for efficient vision based tunnel inspection. In *2015 IEEE International Conference on Intelligent Computer Communication and Processing (ICCP)*. Institute of Electrical and Electronics Engineers Inc.: 335–342.
- McCormick, N. 2010. *NPL REPORT MAT 42 Alternative Methods for Railway Tunnel Examination - A Review and Recommendations*. <https://eprintspublications.npl.co.uk/5049/> 10 August 2022.
- Montero, R., Victores, J.G., Martínez, S., Jardón, A. & Balaguer, C. 2015. Past, present and future of robotic tunnel inspection. *Automation in Construction*, 59: 99–112.
- NR. 2016. *NR_L3_CIV_006_4C - Structures, Tunnels and Operational Property Examinations: Recording of Tunnel Condition Marking Index (TCMI)*.
- Paraskevopoulou, C., Dallavalle, M., Konstantis, S., Spyridis, P. & Benardos, A. 2022. Assessing the failure potential of tunnels and the impacts on cost overruns and project delays. *Tunnelling and Underground Space Technology*, 123: 104443.
- Roerdink, J.B.T.M. & Meijster, A. 2000. The watershed transform: definitions, algorithms and parallelization strategies. *Fundamenta Informaticae*, 41(1–2): 187–228.
- Ronneberger, O., Fischer, P. & Brox, T. 2015. U-Net: Convolutional Networks for Biomedical Image Segmentation. In *Medical Image Computing and Computer-Assisted Intervention – MICCAI 2015*. Munich: 234–241. <http://lmb.informatik.uni-freiburg.de/> 29 March 2022.
- Spencer, B.F., Hoskere, V. & Narazaki, Y. 2019. Advances in Computer Vision-Based Civil Infrastructure Inspection and Monitoring. *Engineering*, 5(2): 199–222.
- Stent, S., Gherardi, R., Stenger, B., Soga, K. & Cipolla, R. 2016. Visual change detection on tunnel linings. *Machine Vision and Applications*, 27(3): 319–330.
- Strauss, A., Bien, J., Neuner, H., Harmening, C., Seywald, C., Österreicher, M., Voit, K., Pistone, E., Spyridis, P. & Bergmeister, K. 2020. Sensing and monitoring in tunnels testing and monitoring methods for the assessment of tunnels. *Structural Concrete*, 21(4): 1356–1376.
- Wang, N., Zhao, Q., Li, S., Zhao, X. & Zhao, P. 2018. Damage Classification for Masonry Historic Structures Using Convolutional Neural Networks Based on Still Images. *Computer-Aided Civil and Infrastructure Engineering*, 33(12): 1073–1089. <https://onlinelibrary.wiley.com/doi/full/10.1111/mice.12411> 22 July 2022.
- Xu, X. & Yang, H. 2020. Vision Measurement of Tunnel Structures with Robust Modelling and Deep Learning Algorithms. *Sensors*, 20(17): 4945. www.mdpi.com/journal/sensors.
- Xue, Y., Xu, T., Zhang, H., Long, R. & Huang, X. 2017. SegAN: Adversarial Network with Multi-scale \mathcal{L}_1 Loss for Medical Image Segmentation. *Neuroinformatics*, 16 (3–4):383–392. <http://arxiv.org/abs/1706.01805> 18 October 2022.
- Yoon, J.S., Sagong, M., Lee, J.S. & Lee, K. 2009. Feature extraction of a concrete tunnel liner from 3D laser scanning data. *NDT & E International*, 42(2): 97–105.
- Zhou, M., Cheng, W., Huang, H. & Chen, J. 2021. A Novel Approach to Automated 3D Spalling Defects Inspection in Railway Tunnel Linings Using Laser Intensity and Depth Information. *Sensors (Basel, Switzerland)*, 21 (17):5725. <https://pmc/articles/PMC8434528/> 1 March 2022.